



University of Utah

UNDERGRADUATE RESEARCH JOURNAL

**DEVELOPMENT AND CHARACTERIZATION OF
INTERCONNECTED POROSITY AEROGELS**

By Alexander Reifsnyder, Mentored by Krista Carlson

Department of Metallurgical Engineering

ABSTRACT

Although silica aerogels have long been tempting materials for filtration media, the closed-cell structure of silica aerogels has prevented this occurrence. By creating a macroscopically open-cell structured silica aerogel, this project seeks to make aerogels viable filtration media. Two different methods were developed to generate silica aerogel membranes using nitrocellulose scaffolds. The first method involved incorporating fibers of nitrocellulose into the sol gel prior to gelation. Nitrocellulose fibers were either removed via calcining after supercritical drying or via a solvent during aging to produce reticulated micron-sized channels in the aerogels. The second method refined the dissolution approach by using a nitrocellulose lacquer mixed with the sol. This mixture separated into two phases, one which was nitrocellulose-rich and the other which was sol-rich. The nitrocellulose-rich phase was subsequently removed from the aerogel using a solvent, creating aerogels with interconnected porosity.

TABLE OF CONTENTS

ABSTRACT	ii
ACKNOWLEDGEMENTS	1
INTRODUCTION	2
METHODS	5
<i>Sol Formation</i>	5
<i>Solvent Exchanges</i>	6
<i>Supercritical Drying</i>	7
<i>Formation of Nitrocellulose</i>	9
<i>Interconnected Porosity Adjustments</i>	10
<i>Silver Nanoparticle Doping</i>	11
<i>Rapid Solvent Exchanges</i>	12
RESULTS	14
<i>SEM Morphology</i>	14
<i>Structural Damage</i>	16
<i>FTIR of Nitrocellulose</i>	17
<i>TEM Analysis</i>	18
<i>Porosity Analysis</i>	20
DISCUSSION	21
CONCLUSION	23
REFERENCES	24

ACKNOWLEDGEMENTS

I gratefully acknowledge the financial support provided by the Crus Center for Renewable Energy for undergraduate student support, the Office for Undergraduate Research, and the U.S. Department of Energy Waste Treatment and Immobilization Plant Project, grant contact number DE-EM0004744.

I also want to thank my parents for fostering my love of research and experimentation.

My interest in science was also supported by several of my teachers. I want to specifically thank Mr. Josephson, Ms. Davis, Ms. Leahy, Dr. Zung, and Mr. Krajca.

INTRODUCTION

Aerogels are a class of ultra-high porosity materials which are composed of a continuous three-dimensional network of meso- and micro-porous structures [1]. Silica aerogels have been thoroughly characterized and considered for innumerable applications that require high chemical durability and extraordinary temperature resilience [2,3]. A typical silica aerogel is hydrophilic but can be modified to become hydrophobic by hybridizing the inorganic framework with various organic cross linkers or polymers. These chemistry adjustments can also increase the mechanical robustness [4–8]. The extremely high surface area of silica aerogel materials make them appear ideal for the filtration of unwanted species from gases, but some issues prevent this process. One of the challenges hindering silica aerogel use in gas filtration applications is the isolated micro-scale porosity of the structural framework, making them nearly impermeable to gases. Even though some solutions have been proposed to circumvent the low permeability issues [9,10], the extremely low density makes implementation of aerogels into real-world applications challenging. Issues such as channeling and other forms of non-uniform flow, as well as difficulties with maintenance [11,12] still plague packed-bed type systems. Adjusting the permeability of silica-based aerogels could enable their use as membranes, eliminating some of the issues faced by these packed-bed systems. Prior studies have focused on altering the sol-gel chemistry to produce aerogel structures with increased permeability to gases [13]. One method to increase the permeability of a monolithic aerogel while maintaining the structural integrity is by introducing meso- or macro-scale interconnected porosity within the microporous matrix [14,16,17]. In some cases,

alteration of the gel chemistry and aging can be performed to decrease in the micropores and increase the mesopores. The resulting aerogels, however, tend to be extremely fragile and more susceptible to fracture during exposure to the higher flow rates observed in many commercial applications [14,15]. Certain organic aerogels have relied on the polarity of two phases in order to produce separate phases during gelation. The polarity difference also allows for easy removal of the unwanted scaffold phase to create voids in the final material [18]. Indeed, numerous reports on this technique have been presented, however none discuss a way to apply this method with inorganic aerogels, such as silica aerogels [7,19,20]. This study describes a new method to produce silica-based aerogel membranes with increased gas permeability by using removable nitrocellulose scaffolds. Nitrocellulose was chosen as the scaffold material due to the ability to disperse nitrocellulose in sols and its ease of removal from the silica matrix by either calcination or dissolution. In addition, nitrocellulose was previously used with excellent results as a template, in combination with surfactants, for the preparation of nanoporous thin films and ceramics [21,22]. In this work, to form membranes with interconnected channels, nitrocellulose fibers were placed directly into the sols during gelation. If the solvent exchange before supercritical drying was performed in ethanol, then the scaffold was removed via calcining the aerogel at 225 °C. However, if acetone was used during the solvent exchange, the nitrocellulose fibers would dissolve, leaving an open channel structure that remained after supercritical drying. Additionally, a highly permeable membrane with interconnected porosity was made using a nitrocellulose lacquer which was mixed with the sol before gelation. Similar to the fiber method, an acetone solvent

exchange could be used to dissolve away the lacquer phase, leading to a highly permeable membrane with interconnected porosity. After creating a highly permeable aerogel, the structure must be functionalized in order to act as an efficient filter. This study functionalized the aerogels with silver nanoparticles, which can be used to capture iodine very effectively. These nanoparticles were produced in-situ by converting silver ions to silver nanoparticles via exposure to ultraviolet light. This thesis elaborates on a previously published work co-authored with Bonan Wang [23].

METHODS

Sol Formation

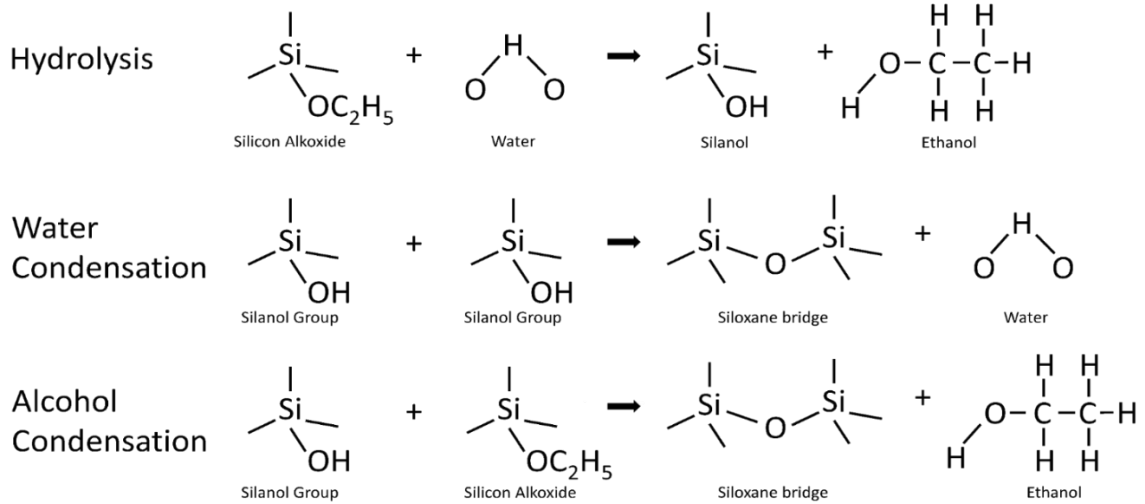


Figure 1. Aerogel formation reactions.

Sol-gels were made using the alkoxy silane precursor tetraethyl orthosilicate. A total of 7 mL of the desired precursor solution was mixed with 11 mL of anhydrous ethanol. A second solution was prepared by mixing 11 mL of anhydrous ethanol, 3 mL of deionized water, 0.0102 mL of ammonium hydroxide, and 0.0246 g of ammonium fluoride. This solution was mixed using a vortex mixer for 30 seconds before adding them to the mold. If the time for gelation was longer than 5 minutes, the molds were gently sealed with parafilm.

Optionally, the tetraethyl orthosilicate can be substituted with a mixture of methyltriethoxysilane and tetraethyl orthosilicate. The addition of this component can significantly alter the final aerogel's mechanical properties and has the added benefit of

making the aerogels hydrophobic. An aerogel with 25 vol% methyltriethoxysilane can be placed directly in a beaker of water and remain intact.

Solvent Exchanges

The solvent exchanges are a straightforward procedure. After the alcogels have solidified, they are immersed in ethanol or a similar solvent to remove impurities. This process is diffusion-limited. Every one milliliter of alcogel requires 25 milliliters of ethanol to exchange. The ethanol is replaced entirely every 18 hours for a total of between 72 and 144 hours.

Supercritical Drying

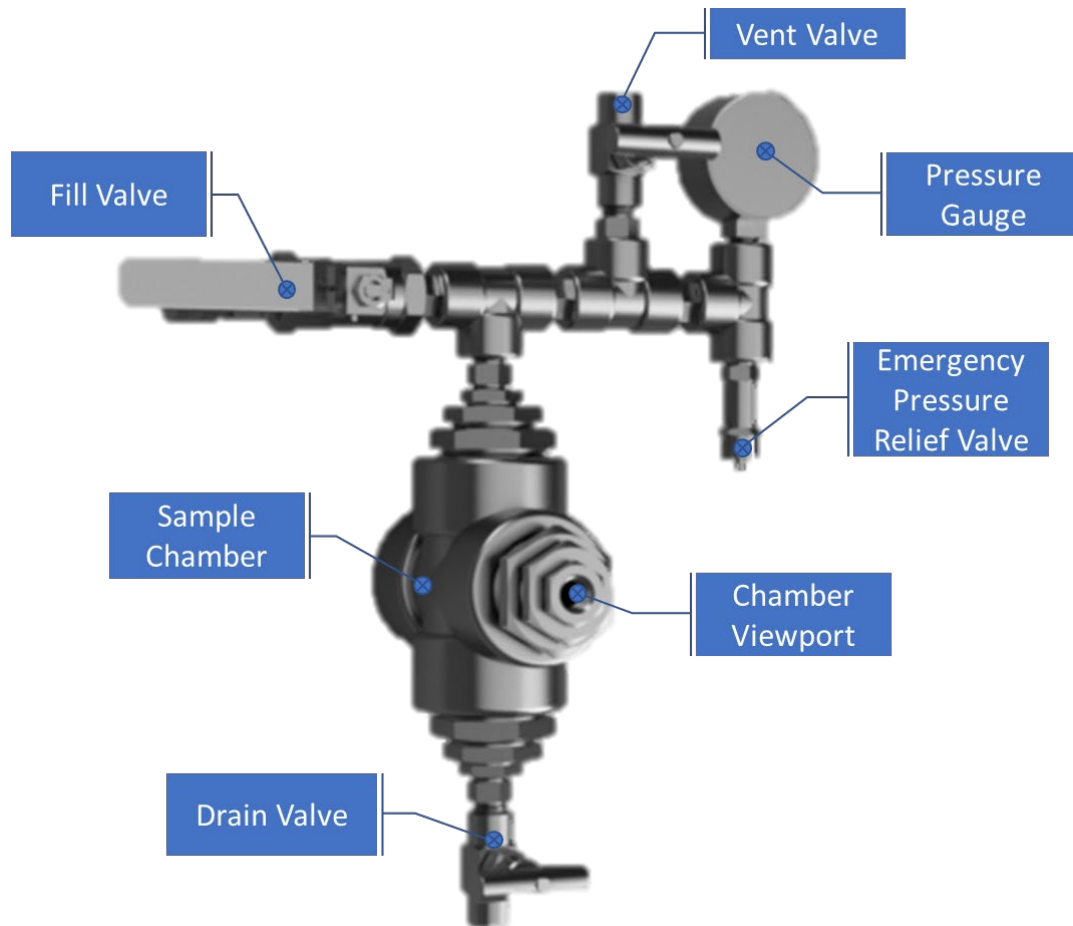


Figure 2. Schematic of the supercritical drying chamber

After solvent exchanging for the prescribed amount of time, the supercritical drying process must begin. Due to the restrictively high price of commercial supercritical dryers, an inexpensive laboratory scale version was constructed out of Class 3000 steel pipe fittings. A three-dimensional rendering of the chamber is displayed in Figure (2). The sample chamber is opened and sealed with the solid plug at the rear of the chamber. On

the opposing face, a viewport allows the chamber to be observed to ensure it is operating correctly.

To load the supercritical dryer, approximately 150mL of solvent is added to the dryer.

Alcogels are then added to the dryer and the dryer is sealed using a pipe plug and Teflon sealant tape. The supercritical dryer is then charged with liquid carbon dioxide through the fill valve. The pressurization rate for the charging process must not exceed 100

PSI/min. This reduces the risk of cracking the alcogels with a severe pressure shock.

After pressurizing, the solvent is drained through the drain valve while the fill valve remains open to replace the drained solvent with liquid carbon dioxide.

After the supercritical dryer is loaded, the solvent in the gels is slowly exchanged with liquid carbon dioxide. The process to exchange the supercritical dryers is to first open the fill valve, then the vent valve is gently cracked open. The drain valve is opened until approximately one pound of carbon dioxide has been exchanged. This can be measured via weighing the dry ice as it exits the supercritical dryer or by measuring the weight lost from the syphon tank. The solvent exchange process is repeated three times, with 24 hours between each exchange.

Supercritical drying is achieved by heating the supercritical drying chamber through its critical point. Due to the closed nature of the chamber, the heating process causes the pressure to increase. The vent valve is opened to relieve excess pressure. Due to the design limitations, the pressure in the supercritical drying chamber must not exceed 2,000 PSI but during supercritical drying the pressure must not be lower than 1,100 PSI. There is a safety valve which is calibrated to release pressure when the supercritical drying

chamber reaches 2,000 PSI. The chamber is heated until the internal temperature reaches 45 degrees Celsius, as verified by an infrared thermometer pointed at the sight glass on the chamber. Once the internal temperature has reached this threshold, the chamber is isothermally depressurized by opening the vent valve while heating the chamber. The rate of depressurization must not exceed 100 PSI/min. This reduces the risk of cracking the aerogels with a severe pressure shock.

Formation of Nitrocellulose

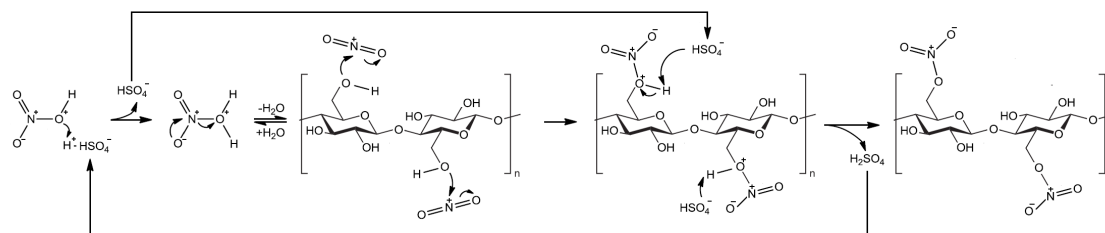


Figure 3. Esterification of cellulose

Nitrocellulose was formed by nitrating cellulose in the form of cotton balls in a 40 °C mixture of 75 mL sulfuric acid and 25 mL nitric acid. Approximately 400mg of cellulose was placed in the nitration solution and allowed to react for various time periods between 10 and 60 minutes. During this reaction, sulfuric acid acts as both a desiccant and a catalyst by removing water from the reaction and providing H^+ to the HNO_3 to generate the active nitrating agent, NO_2^+ . 10 minutes was the shortest nitration time period used for this project. Cotton which was nitrated for less than 10 minutes burned similarly to the original cotton and had very limited solubility in acetone. After nitration, the nitrocellulose was washed in a bath of chilled deionized water. The nitrocellulose was

washed for a total of 15 minutes, replacing the entirety of the water every five minutes. Sodium bicarbonate was added to the final bath to ensure neutralization of excess acid. The washed nitrocellulose was dried at for 12 hours at 60 °C in a drying oven located in a fume hood. Due to the risk of spontaneous combustion which is associated with nitrocellulose, the samples were used immediately after the completion of the drying process to eliminate the need for storage.

Interconnected Porosity Adjustments

To create the interconnected porosity, two methods were explored. First, 7-25 milligrams of nitrocellulose fibers (a 'scaffold') were evenly dispersed throughout the mold. The sol was then allowed to set while the fibers remained in place. The scaffold could then be removed during solvent exchanging by replacing the solvent with acetone. Lengthening the solvent exchange time to 144 hours is necessary in order to fully remove the fibers. The sol gel is then supercritically dried according to standard procedure. Alternatively, the fibers could be removed after supercritical drying. In this procedure, the sol is solvent exchanged for the standard 72 hour period, then supercritically dried. After the aerogels were removed from the supercritical drying chamber, they were calcined in pure oxygen at 220 degrees Celsius to remove the scaffold.

The second procedure uses a mixture of nitrocellulose and acetone. For every 25 milligrams of nitrocellulose, 1 milliliter of acetone is used. This 'lacquer' is then dispersed in the sol by vortex mixing for one minute. The resulting mixture separates into

microdroplets of lacquer and, after the sol gel sets, the lacquer can be removed by solvent exchanging in acetone for 144 hours. This lacquer cannot be removed with calcining.

Silver Nanoparticle Doping

Silver nanoparticles can be introduced into the aerogel by adding 2.2 grams of silver nitrate to the sol. This is best accomplished by first dissolving the silver nitrate in the water used for making the sol, then adding the water to the rest of the mixture. This ensures that all the silver nitrate dissolves and is evenly distributed throughout the sol. During curing, the sol is exposed to ultraviolet lights to convert the silver nitrate into silver nanoparticles. UV-C lamps were used to expose the gel over an eight-hour period. Following this, the gels were processed according to standard procedures.

Rapid Solvent Exchanges

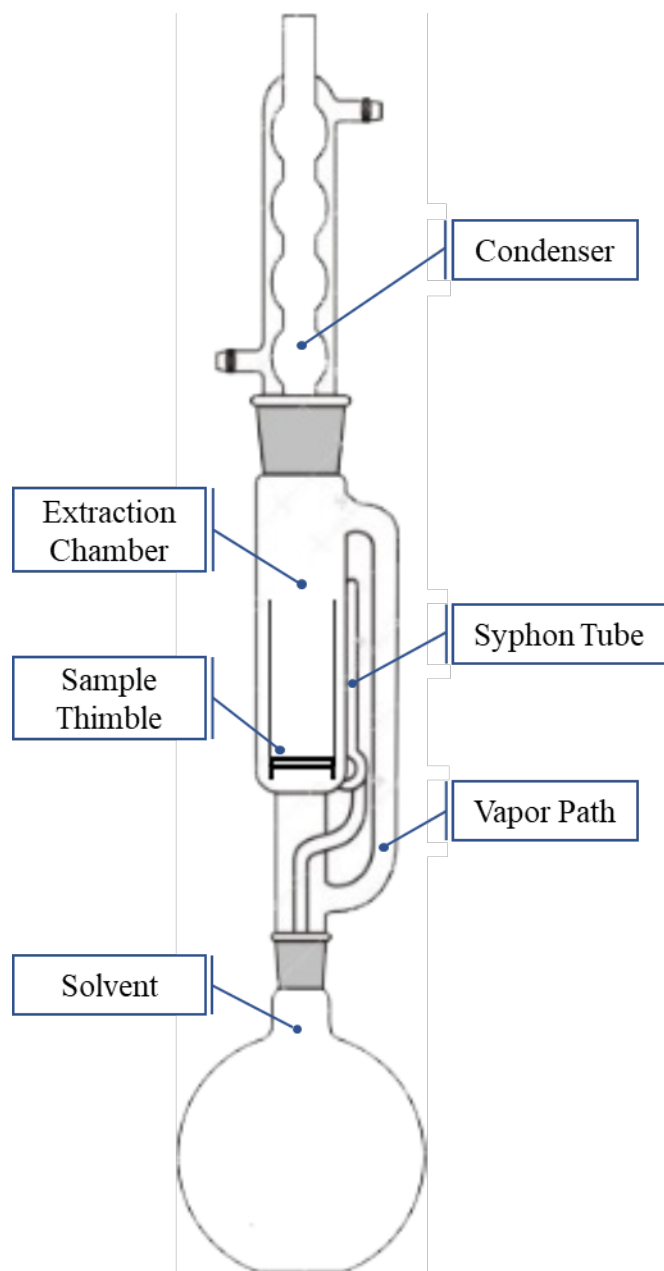


Figure 4. A Soxhlet extraction apparatus [24]

With the adjustments to the formation procedure introduced by the interconnected porosity process, the lengthy solvent exchanges were causing a bottleneck in testing. Therefore, a faster method of solvent exchanging was sought. A Soxhlet extractor is a special piece of glassware which continuously exposes a sample to a hot solvent, periodically replacing and draining the used solvent. This procedure not only decreases the time needed to exchange the alcogels, it also reduces the amount of solvent used for the process. The Soxhlet extractor we used has a 150mL capacity in the extraction chamber, and has a solvent period of approximately 10 minutes. By using the Soxhlet extractor to perform the solvent exchanges, the exchange time for all alcogels has been reduced to 24 hours.

RESULTS

SEM Morphology

The microstructure aerogels were characterized using a Hitachi S-4800 scanning electron microscope. Tetraethyl orthosilicate-based aerogels (TEOS) and Methyltriethoxysilane (MTES) hybridized aerogels were tested with varied levels of loading, both for the fiber process and for the nitrocellulose lacquer.

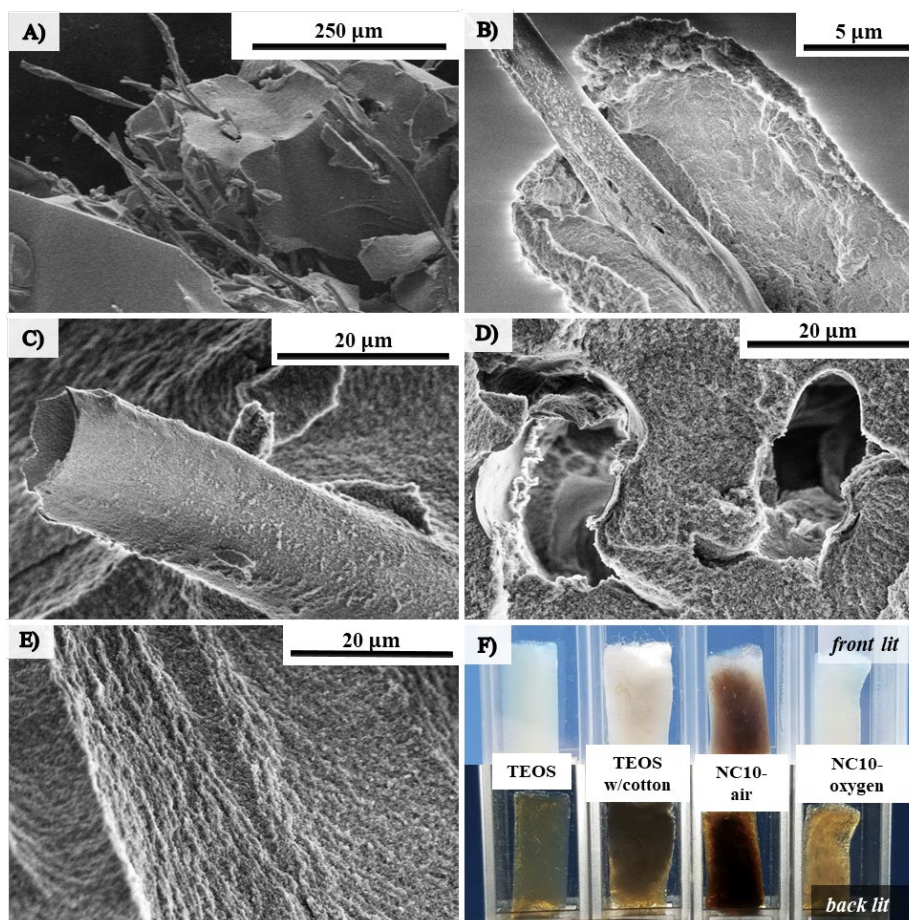


Figure 5. Tetraethyl orthosilicate aerogel membranes formed using the calcining method. Nitrocellulose scaffold was still present after calcining in oxygen at 225 °C (A). Fibers which remained present in the membrane after calcining in air (B) were removed after recalcining in oxygen at 500 °C (C, D). The channel linings show the same structure as the surrounding aerogel (E). Photographs of different aerogels and the result of nitrocellulose removal via calcination in air versus oxygen (F).

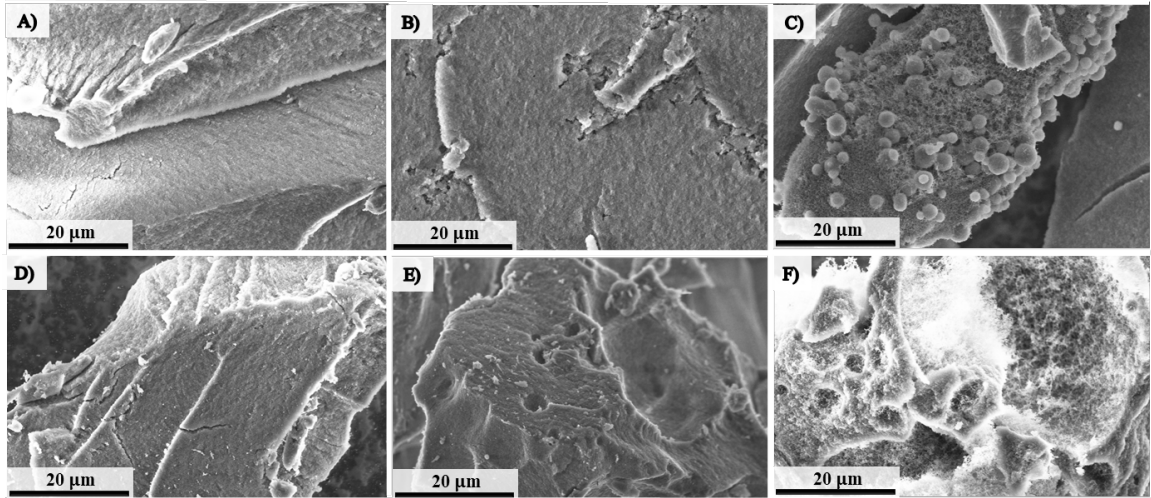


Figure 6. TEOS based membranes with 25, 33, and 50 percent lacquer (A,B,C). MTES based membranes with 25, 33, and 50 percent lacquer (D,E,F).

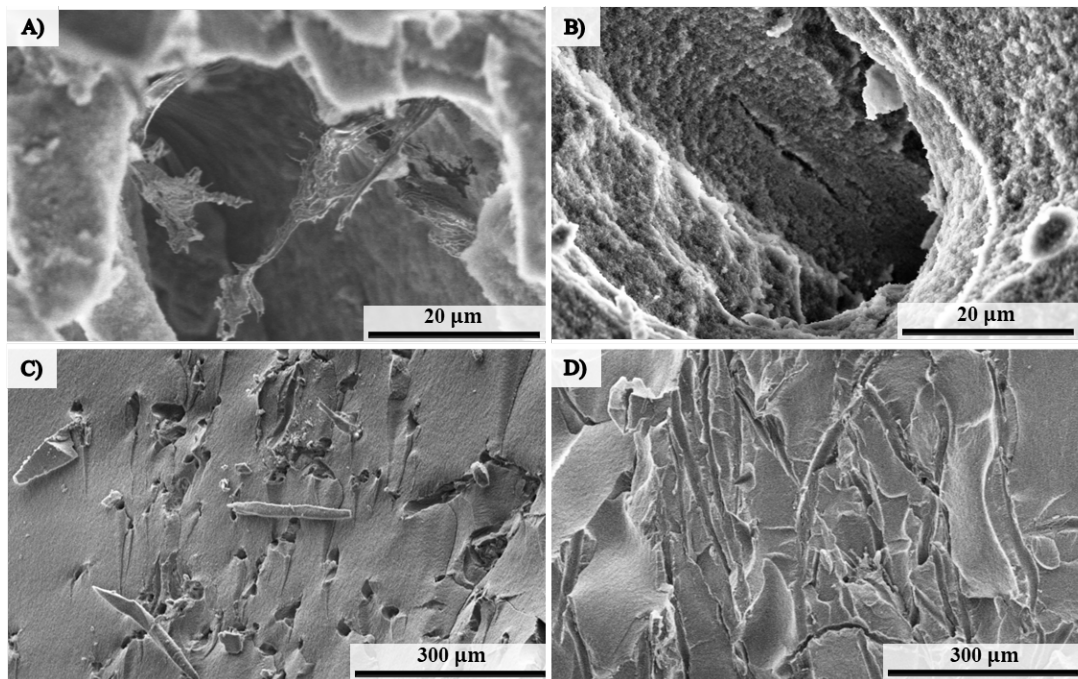


Figure 7. MTES aerogels fabricated with nitrocellulose fibers solvent exchanged in acetone before supercritical drying. The acetone exchange dissolved most of the 30 minute fibers (A) and all 60 minute nitrocellulose fibers (B) The dissolution of the nitrocellulose scaffold leaves interconnected channels on the order of tens of microns (C,D).

Structural Damage

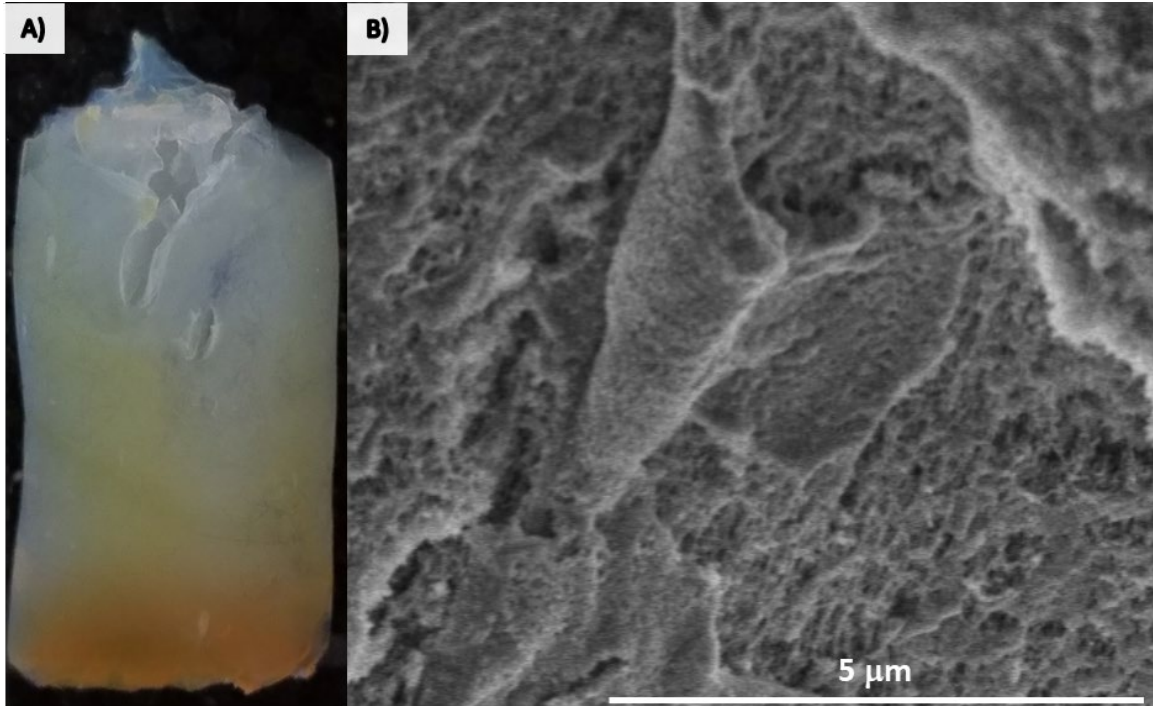


Figure 8. Aerogels produced with the calcination method can become damaged from heat (A). (B) shows the microstructure from the top portion of the aerogel.

FTIR of Nitrocellulose

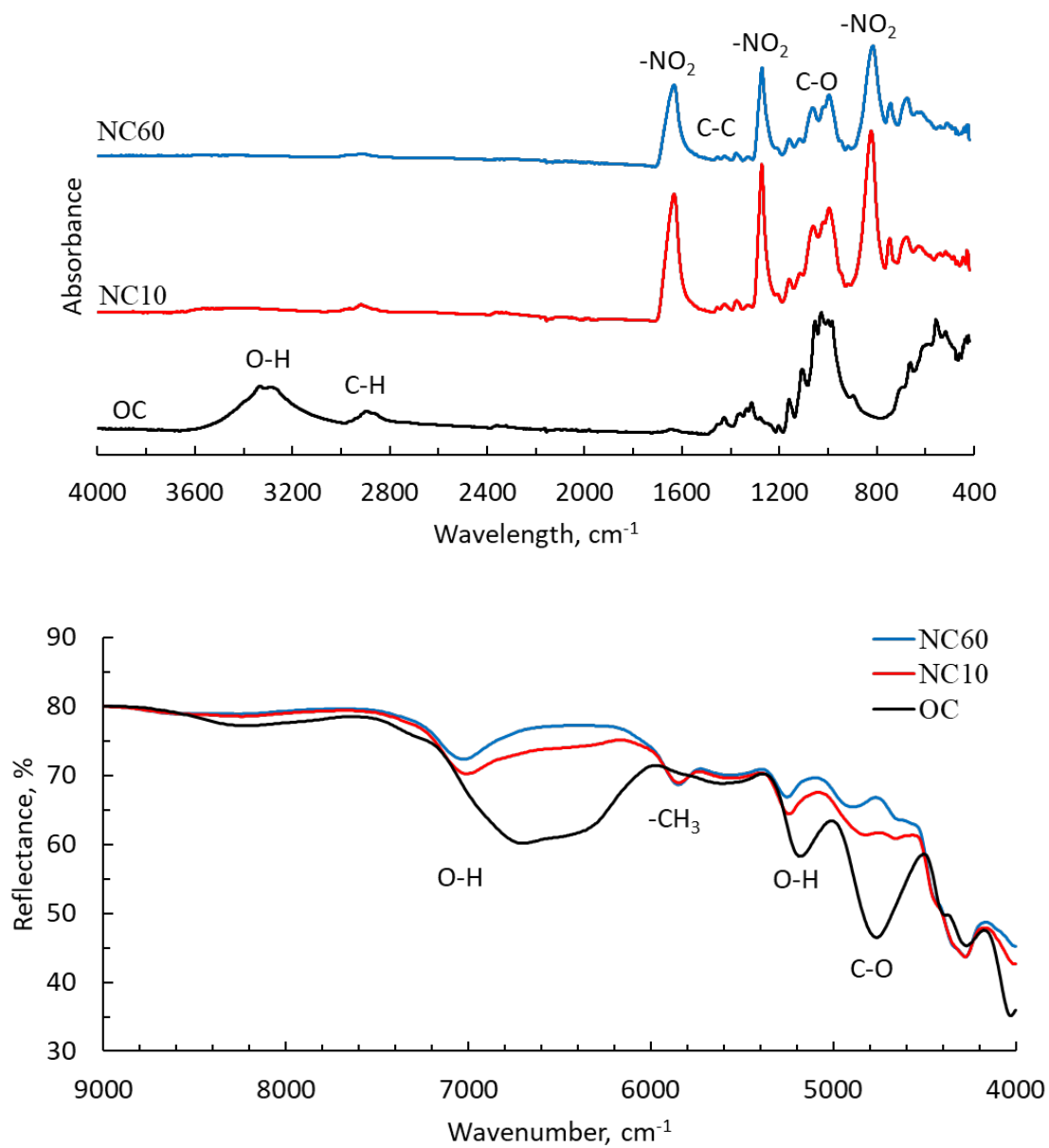


Figure 9. FTIR of nitrocellulose and cotton (Top). NIR of nitrocellulose and cotton (Bottom).

TEM Analysis

Transmission electron microscopy was performed to ensure that the sample contained silver nanoparticles which were free of oxides. This TEM was performed with a Joel JEM 2800 S/TEM.

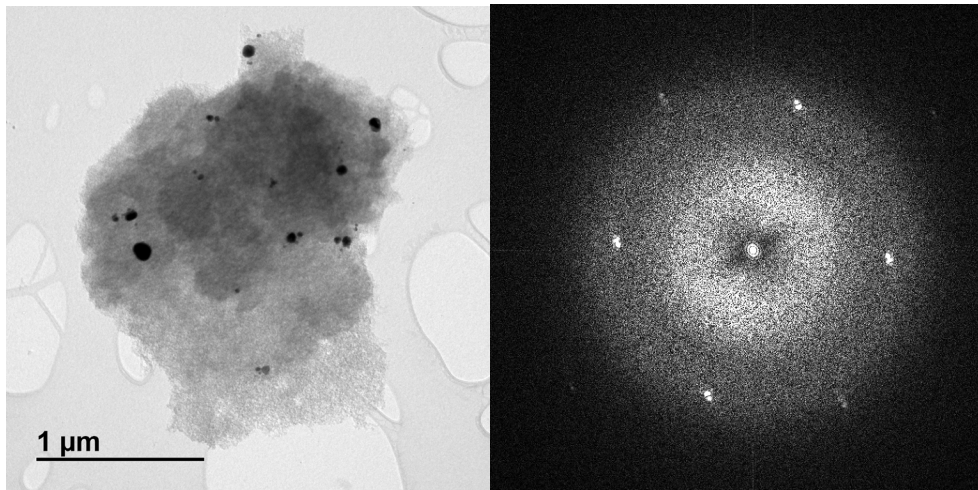


Figure 10. TEM micrograph of a silica aerogel chunk with nanometer-sized silver particles (Left) and a diffraction pattern showing a crystalline structure of the nanoparticles (right)

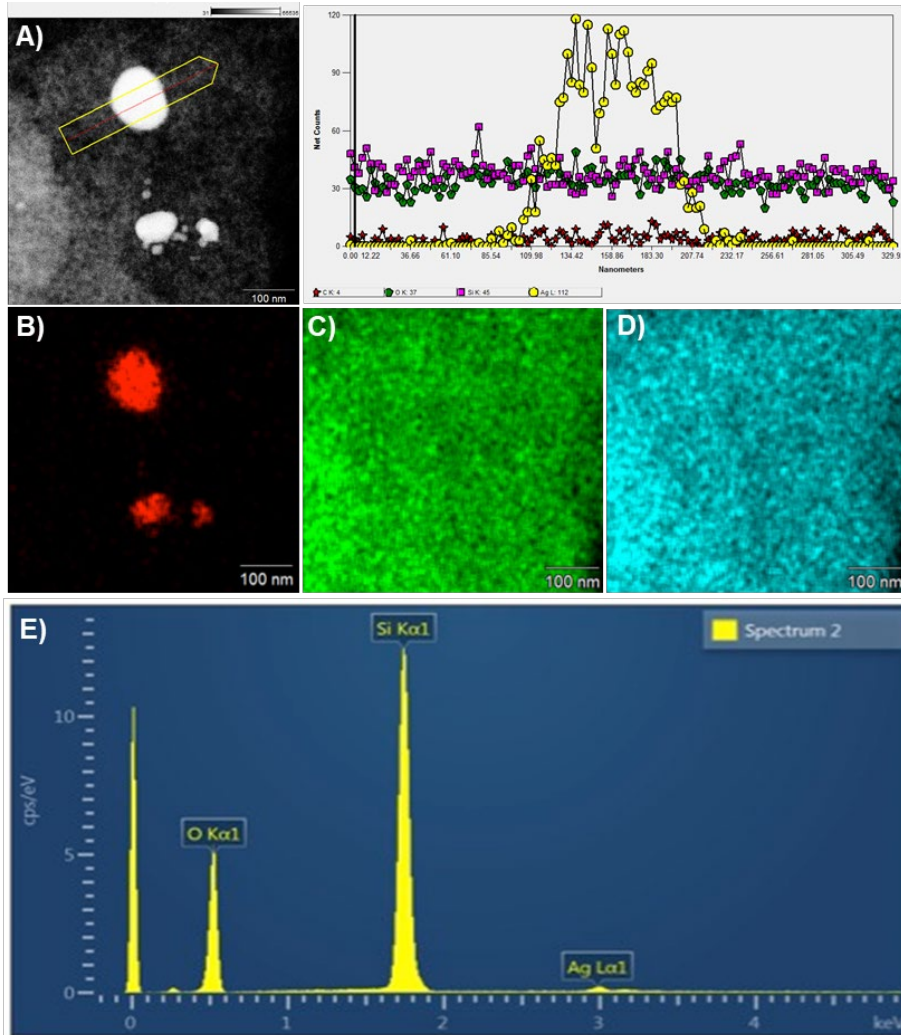


Figure 11. The line EDX analysis of a silver nanoparticle where silver is yellow (A). A full EDX analysis of silver (B), silicon (C), oxygen (D) and the relative abundance of each (E)

Porosity Analysis

Sample	Bulk density, ρ_b (g/cm ³)	Skeletal density, ρ_s (g/cm ³)	Shrinkage (%)	Closed porosity (%)	He permeability (x10 ⁻¹⁰ m ²)
T-0	0.0378 ± 0.0005	0.3903 ± 0.0010	0 ± 0	90	1.940 ± 0.005
T-25	0.0436 ± 0.0001	0.3333 ± 0.0002	11 ± 3	87	3.918 ± 0.024
T-33	0.0472 ± 0.0002	0.2915 ± 0.0003	7 ± 3	84	5.104 ± 0.015
T-50	0.0588 ± 0.0002	0.2743 ± 0.0002	3 ± 3	79	8.433 ± 0.077
M-0	0.0340 ± 0.0003	0.4653 ± 0.0006	27 ± 3	93	2.503 ± 0.012
M-25	0.0340 ± 0.0002	0.3848 ± 0.0003	37 ± 3	91	4.511 ± 0.146
M-33	0.0343 ± 0.0003	0.3616 ± 0.0006	33 ± 3	91	5.705 ± 0.018
M-50	0.0469 ± 0.0004	0.3537 ± 0.0008	29 ± 3	87	12.122 ± 0.022

Table 1. Helium pycnometry data for a variety of TEOS AND MTES samples. T-xx is coded for a TEOS aerogel with xx% lacquer. M-xx is coded for a MTES aerogel with xx% lacquer.

DISCUSSION

Initial results showed that the nitrocellulose fibers of the aerogel remained intact after calcination at low temperature, but could be effectively removed from TEOS-based aerogels by calcining in oxygen at a high temperature, shown in Figure (5C) and (5D). Though the structure on the inside of the channels appear consistent in some experiments, such as Figure (5E), the results were sometimes less successful. The white boundaries towards the top of the aerogel shown in Figure (8A) indicate that the high localized heat from the combustion of the nitrocellulose has caused the microstructure to condense. This can be confirmed with Figure (8B) where the structure of the aerogel has clearly been damaged. When the nitrocellulose was removed with an acetone solvent exchange, the channel lining appeared more compact than the bulk aerogel as can be seen in Figure (7B). While simple, the use of fibers had issues with damage and consistency whether dissolution or calcination was used.

The development of the nitrocellulose lacquer method showed great improvement in consistency and possible loading levels. Figure (6) shows a series of aerogel samples produced with the lacquer method. In the TEOS aerogels, shown in Figures (6A), (6B), and (6C), increased mesopores and pitting of the aerogels with increasing lacquer content occurs. A similar phenomenon can be observed with MTES aerogels shown in Figures (6D), (6E), and (6F). These MTES samples appear to have more cohesive and homogenous microstructures than the equivalent TEOS samples, creating fine web-like structures rather than large isolated pitting. This phenomenon is especially apparent in the comparison between Figure (6C) and (6F).

The nitrocellulose used to produce these aerogels has been optimized to provide optimal solubility in acetone yet remain insoluble in ethanol. The FTIR and NIR data displayed in Figure (9) shows that esterification of cotton readily takes place. The nitrogen content of the nitrocellulose used in this study is expected to be greater than 11.3%. It has been reported that when the nitrogen content is between 10.7%–11.3%, nitrocellulose is reportedly soluble in alcohols, ketones, esters, and glycol ethers, but at nitrogen contents greater than 11.3% the nitrocellulose is no longer soluble in ethanol [25].

Silver nanoparticles were produced and confirmed to be in the matrix of the aerogel with TEM analysis. Figure (10) shows a small silica monolith with nanoscale silver embedded in it and a diffraction pattern suggesting that the nanoparticles are crystalline in nature.

The lack of oxides on these nanoparticles was confirmed with the EDX data presented in Figure (11).

The helium pycnometry data presented in Table (1) shows that with increasing percentages of lacquer, the porosity increases. The MTES aerogels were generally more permeable, which is consistent with the observations from Figure (6).

CONCLUSION

This thesis examined the process of creating interconnected porosity aerogels via two unique methods. Both methods improved gas permeability through the monolithic aerogel. While incorporating nitrocellulose fibers directly into the aerogels did produce interconnected porosity, the removal of the fibers was inconsistent and often led to damage to the microstructure of the aerogel. Making aerogels with the lacquer scaffold was by far the more effective approach. The MTES-based aerogel with 50% nitrocellulose lacquer was the most permeable aerogel produced in this study, and it was also the most consistent in microstructure and repeatability. One of the many benefits to this process is the potential to be applied to a wide range of aerogel chemistries. With the new ability to use monolithic forms as a filtration media, aerogels may soon find new uses in society.

REFERENCES

- [1] M. Anderson, R. Stroud, C. Morris, C. Merzbacher, D. Rolison, Tailoring advanced nanoscale materials through synthesis of composite aerogel architectures, *Adv. Eng. Mater.* 2 (2000) 481–488.
- [2] K. Sinkó, Influence of chemical conditions on the nanoporous structure of silicate aerogels, *Materials* 3 (2010) 704.
- [3] Z. Ülker, D. Sanli, C. Erkey, Chapter 8 - applications of aerogels and their composites in energy-related technologies, in: V. Anikeev, M. Fan (Eds.), *Supercritical Fluid Technology for Energy and Environmental Applications*, Elsevier, Boston, 2014, pp. 157–180.
- [4] K. Kanamori, Y. Kodera, G. Hayase, K. Nakanishi, T. Hanada, Transition from transparent aerogels to hierarchically porous monoliths in polymethylsilsesquioxane sol-gel system, *J. Colloid Interface Sci.* 357 (2011) 336–344.
- [5] S. Li, H. Ren, J. Zhu, Y. Bi, Y. Xu, L. Zhang, Facile fabrication of superhydrophobic, mechanically strong multifunctional silica-based aerogels at benign temperature, *J. Non-Cryst. Solids* 473 (2017) 59–63.
- [6] A. Mahani, S. Motahari, A. Mohebbi, Sol-gel derived flexible silica aerogel as selective adsorbent for water decontamination from crude oil, *Mar. Pollut. Bull.* 129 (2018) 438–447.
- [7] H. Maleki, L. Duraes, A. Portugal, A new trend for development of mechanically robust hybrid silica aerogels, *Mater. Lett.* 179 (2016) 206–209.
- [8] S. Standeker, Z. Novak, Z. Knez, Adsorption of toxic organic compounds from water with hydrophobic silica aerogels, *J. Colloid Interface Sci.* 310 (2007) 362–368.
- [9] M. Guise, B. Hosticka, B. Earp, P. Norris, An experimental investigation of aerosol collection utilizing packed beds of silica aerogel microspheres, *J. Non-Cryst. Solids* 285 (2001) 317–322.
- [10] N. Soelberg, T. Watson, Deep bed adsorption testing using silver-functionalized aerogel, in: D.o.E.N. Laboratory (Ed.), *Idaho National Laboratory*, 2012.
- [11] A. Kohl, Absorption and stripping, in: R. Rousseau (Ed.), *Handbook of Separation Process Technology*, Wiley & Sons, 1987.
- [12] R. Perry, D. Green, *Perry's Chemical Engineers' Handbook*, 7 ed., McGraw Hill, 1997.
- [13] S. Cao, K. Yeung, J. Kwan, P. To, S. Yu, An investigation of the performance of catalytic aerogel filters, *Appl. Catal. B Environ.* 86 (2009) 127–136.
- [14] M. Aegerter, N. Leventis, *Aerogels Handbook*, Springer, 2011.
- [15] R. American Society of Heating, A.-C. Engineers, 2005 ASHRAE Handbook: Fundamentals, ASHRAE, 2005.
- [16] S. Gu, S. Jana, Open cell aerogel foams with hierarchical pore structures, *Polymer* 125 (2017) 1–9.
- [17] J. Korhonen, P. Hiekkataipale, J. Malm, M. Karppinen, O. Ikkala, R. Ras, Inorganic hollow nanotube aerogels by atomic layer deposition onto native nanocellulose templates, *ACS Nano* 5 (2011) 1967–1974.

- [18] X. Wang, S.C. Jana, Tailoring of morphology and surface properties of syndiotactic polystyrene aerogels, *Langmuir* 29 (2013) 5589–5598.
- [19] S.J. Kim, P. Raut, S.C. Jana, G. Chase, Electrostatically active polymer hybrid aerogels for airborne nanoparticle filtration, *ACS Appl. Mater. Interfaces* 9 (2017) 6401–6410.
- [20] N. Teo, S.C. Jana, Open cell aerogel foams via emulsion templating, *Langmuir* 33 (2017) 12729–12738.
- [21] X. Li, G. Fryxell, C. Wang, J. Young, Nitrocellulose templated hierarchical pore structure in mesoporous thin films, *Inorg. Chem. Commun.* 9 (2006) 7–9.
- [22] X. Li, G. Fryxell, C. Wang, J. Young, Templating mesoporous hierarchies in silica thin films using the thermal degradation of cellulose nitrate, *Microporous Mesoporous Mater.* 99 (2007) 308–318.
- [23] Wang, B., Reifsnnyder, A., Zharov, I., & Carlson, K. (2019). Silica aerogel membranes fabricated using removable nitrocellulose scaffolds. *Microporous and Mesoporous Materials*, 278, 435-442. doi:10.1016/j.micromeso.2018.12.045
- [24] “Soxhlet Extraction.” *Indiamart* www.indiamart.com/proddetail/soxhlet-extraction-19701915748.html.
- [25] Nitrocellulose Walsroder Nitrocellulose: Essential for an Extra-special Finish, DOW Chemical Company

Name of Candidate: Alexander Reifsnyder
Birth date: March 17, 1997
Birth place: Port Chester, New York
Address: 747 Boston Post Road
Rye, NY 10580